The Cyanobacterial Repressor SmtB Is Predominantly a Dimer and Binds Two Zn^{2+} Ions per Subunit†

Sambit R. Kar,‡ Amy C. Adams,§ Jacob Lebowitz,|| Kenneth B. Taylor,§ and Leo M. Hall*,§

The Graduate Program in Biophysical Sciences, Department of Microbiology, and Department of Biochemistry and Molecular Genetics, University of Alabama at Birmingham, Birmingham, Alabama 35294-2041

Received July 11, 1997; Revised Manuscript Received October 9, 1997⊗

ABSTRACT: The *Synechococcus* PCC7942 metallothionein repressor gene *smtB* has been cloned into a high expression vector and the protein purified to near homogeneity (≥98%). Analytical ultracentrifugation studies demonstrate that the protein is predominantly dimeric in 0.1 M NaCl, pH 7.4, and 22 °C, exhibiting a monomer−dimer−tetramer equilibrium. The monomer−dimer ($K_{a(1,2)}$) and the dimer−tetramer ($K_{a(2,4)}$) association constants are 3.24×10^5 and 9.90×10^2 M^{-1}, respectively. The repressor binds two Zn^{2+} ions per subunit with an overall K_d of 3.49×10^{-6} M. In the presence of Zn^{2+}, $K_{a(1,2)}$ increases by 2 orders of magnitude to 1.25×10^7 M^{-1} and the apparent weight-averaged sedimentation coefficient increases from 2.00 to 2.22 S. The fact that the increase in sedimentation coefficient is greater than that predicted by increased dimerization is interpreted as caused by compaction of the structure in the presence of metal ions. At pH 6.0, 0.1 M NaCl, and 22 °C, the protein exhibits only a monomer−dimer equilibrium, with $K_{a(1,2)} = 1.52 \times 10^7$ M^{-1} which is almost identical to that seen upon binding Zn^{2+} at pH 7.4. The compaction and conformational change in SmtB caused by Zn^{2+} is consistent with a role for this altered quaternary state in derepression of *smtA* in *Synechococcus* challenged with heavy metal ions.

In *Synechococcus* PCC7942, tolerance to zinc and cadmium ions is imparted by the *smt* locus of the chromosome as verified by Zn/Cd-intolerant *smt*⁻ mutants that are devoid of this locus (*1*). The *smt* locus consists of two divergently transcribed genes, *smtA* and *smtB*. The former encodes a class II metallothionein of 56 amino acids, designated SmtA. The latter encodes SmtB, a 122 amino acid *trans*-acting repressor of *smtA*. A 100-bp operator/promoter region lies between the *smtA* and the *smtB* protein coding regions, and it contains divergent and overlapping promoters for the two genes (*1*). The promoter for *smtA* contains a pair of sense/antisense sites, designated S1 and S2, within an imperfect 6−2−6 inverted repeat at the *smtA* transcription start site. Another pair of sites, designated S3 and S4, is situated within a 7−2−7 inverted repeat between the −10 sequences of the two divergent genes. Both pairs of sites are contacted by SmtB at the TGAA sequence as deduced from methylation interference assays (*2*). Complete footprints of the repressor at these sites, however, are not known. *Synechococcus* metallothionein synthesis is regulated by heavy metal ions (*3*, *4*). In the absence of metal ions the transcription of *smtA* is repressed while the transcription is enhanced in response to increased concentrations of Zn^{2+}, Cd^{2+}, and to a lesser extent by Cu^{2+}, Hg^{2+}, Co^{2+}, Ni^{2+}, Au^{2+}, and Ag^{+} ions (*4*, *5*).

Cellular extracts of cyanobacteria form complexes with DNA which have been analyzed by electrophoretic mobility shift assay (EMSA)[1] (*1*). Recombinant SmtB forms three distinct complexes with its cognate operator/promoter DNA in the absence of heavy metal ions. Upon electrophoresis the fastest migrating complex, designated C1, forms at the lowest protein concentrations when SmtB binds either S1 or S2. Binding of the repressor at both S1 and S2 generates the slower migrating intermediate complex C2. The slowest migrating complex, designated C3, forms at the highest protein concentrations when both pairs of sites are occupied by the repressor. Simultaneous to the formation of C3, the formation of C1 and C2 is decreased. The formation of all the three DNA−protein complexes is inhibited *in vitro* by Zn^{2+} ions (*2*). Computer analysis of the SmtB sequence has predicted one zinc ion binding site per monomer (*6*). In the event of heavy metal induction, SmtB is proposed to directly bind the metal *in situ*. From site-directed mutagenesis analysis, His105 and/or His106 have been implicated in binding the divalent metal ion while the cysteine residues have not (*7*). However, it has not been established whether one or both of the histidine residues are involved in formation of the metalloprotein complex. Furthermore, neither the stoichiometry of metal ion binding to the repressor nor the thermodynamics and stoichiometry of DNA binding by the repressor has been established.

Recently, the crystal structure of SmtB has been determined (*8*). SmtB purified according to the procedure described here crystallizes as a dimer, free of heavy metal. The axial ratio of the dimer in the metal-free SmtB crystal is 3.3. The dimer has four putative metal binding sites. Two of the sites are formed by residues contributed solely by each

† This work was supported in part by the XL-A Instrumentation Grant BIR-9419624 from the National Science Foundation to J.L., and the National Oceanic and Atmospheric Administration, U.S. Department of Commerce, under Grant NA016RG0155, ProjectE/0-16 and the Mississippi−Alabama Sea Grant Consortium to L.M.H. and K.B.T.

* Author to whom correspondence should be addressed.
‡ The Graduate Program in Biophysical Sciences.
§ The Department of Biochemistry and Molecular Genetics.
|| The Department of Microbiology.

⊗ Abstract published in *Advance ACS Abstracts,* November 15, 1997.

[1] Abbreviations: SDS, sodium dodecyl sulfate; PAGE, polyacrylamide gel electrophoresis; PCR, polymerase chain reaction; PVDF, polyvinylidene fluoride; Tris, tris(hydroxymethyl)aminomethane; Mes, 2-morpholinoethanesulfonic acid; NTA, nitrilotriacetic acid; DTT, dithiothreitol; IPTG, isopropyl thiogalactoside; EDTA, ethylenediaminetetraacetic acid; PEI, polyethylenimine; rms, root mean square; OD, optical density; EMSA, eletrophoretic mobility shift assay.

S0006-2960(97)01690-5 CCC: $14.00

monomer and two other sites are formed by amino acid residues contributed by both monomers at the shared interface between them. The recognition helices of each monomer, subunit can fit into the S1/S2 (or S3/S4) sites provided there is a conformational change in the SmtB dimer or in the DNA operator/promoter region or both.

This paper, therefore, addresses several structural features of SmtB that are relevant for our understanding of the mechanism of the transcriptional control exerted by this repressor. This paper explores (1) the quaternary state(s) of the protein in the absence of DNA, (2) the stoichiometry of Zn^{2+} ion binding by SmtB, and (3) the effect of Zn^{2+} binding on the quaternary state(s) of the protein.

MATERIALS AND METHODS

Chemicals and Molecular Biology Materials. Radioactive $^{65}ZnCl_2$ was obtained from NEN Research Products. Restriction endonucleases and DNA ligase were from Gibco-BRL, and kits for purification of DNA were obtained from Promega. The pET29a(+) vector with appropriate *Escherichia coli* strains were obtained from Novagen. Precast SDS 15% acrylamide gels, SDS, and coomassie R250 were from Bio-Rad. Agarose was from FMC. PCR primers were obtained from IDT, Inc. Ion-exchange and desalting columns or cartridges were from Pharmacia Biotech. Immobilon-P and PVDF membranes were from Millipore. Cassette dialyzers (MWCO 10000) were from Pierce. VivaSpin15 membrane filtration units were from VivaScience. Microbiological media components were from DIFCO. Polyethylenimine (PEI), tris(hydroxymethyl)aminomethane (Tris), 2-morpholinoethanesulfonic acid (Mes), nitrilotriacetic acid (NTA), dithiothreitol (DTT), and isopropyl thiogalactoside (IPTG) were from Sigma or Fisher Scientific. Other chemicals were from Sigma or Fisher Scientific.

Cloning of smtB. The coding region of the *smtB* gene contained in plasmid pJLE3C (*2*) was amplified by PCR with custom-made primers to introduce *Nde*I and *Sal*I restriction sites for subsequent subcloning into pET29a(+) vector according to the manufacturer's instructions. The primers used to introduce the *Nde*I and *Sal*I sites (in italics) were 5′CGTGATTGG*CATATG*ACAAAACCAGTGCTGCAGG3′ and 5′CTACAGCAA*GTCGAC*CAAGAACGATGCC3′, respectively. The gel-purified DNA fragment was then insert-ligated into pET29a(+). NovaBlue cells were transformed with this plasmid construct, and *smtB*-containing colonies were identified by colony-PCR with the same two primers. Positive colonies were further verified by confirming the size of the inserted gene after restriction-digesting their purified plasmid DNA with *Nde*I and *Sal*I endonucleases. Plasmid designated pSRK15-1 isolated from a selected colony was used to transform *E. coli* BL21(DE3) expression host. Cells containing the proper *smtB* insert were selected and maintained at −70 °C in LB medium containing 15% glycerol.

Growth of BL21(DE3)/pSRK15-1. For expression of SmtB in *E. coli* BL21(DE3)/pSRK15-1, a seed culture was prepared in Luria broth containing kanamycin sulfate, 60 mg/L, at 37 °C by inoculation with a fresh colony grown at 37 °C on a 1.5% agar plate with the same medium. A 500 mL inoculum was used to grow cells in 24 L of the same culture medium at the Fermentation Facility at UAB. The cells were grown at 37 °C with vigorous aeration (12 L/min) and stirring (250 rpm) to an OD of 1.5 at 600 nm. The pH was maintained at 7.4 by the addition of NaOH. Expression of SmtB was induced by the addition of IPTG to a concentration of 1.2 mM. Cells were harvested 3 h postinduction by concentration with a Pellicon concentrator (Millipore) fitted with a GVPP membrane filter, followed by centrifugation at 5000*g*. The yield of wet cell paste was approximately 110−120 g. The cell paste was either used immediately or stored at −70 °C for up to several months.

SmtB Purification. Cells, 110 g, were slurried in 1:10 (w/v) of buffer B (25 mM Mes, 2 mM DTT, 1 mM EDTA, pH 6.0) and lysed at 15 000 psi by a single pass through a French press. After adjustment of the pH to 6.0 with 1.0 M HCl, the lysate was centrifuged at 10000*g* for 30 min. The viscous supernatant was collected together with a gelatinous zone of material near the packed precipitate and combined. Protein and nucleic acid were precipitated by the dropwise addition (0.015 v/v of lysate supernatant) of a 10% solution of PEI (previously adjusted to pH 6.0). After stirring 1−2 h, the precipitate was collected by centrifugation at 10000*g* for 30 min. The precipitate was extracted by stirring overnight with 0.5 M NaCl in buffer B (5 mL/g cell paste). After centrifugation at 10000*g* for 30 min, the protein in the supernatant was concentrated by the addition of solid $(NH_4)_2SO_4$ to 3.0 M. The precipitate was collected by centrifugation at 10000*g* and dissolved in 40 mL of buffer B. The solution was dialyzed in 15 mL portions in cassette dialyzers against 1 L of the same buffer. A precipitate that formed during dialysis was removed by centrifugation at 10000*g*. The above operations were performed at 4 °C, whereas the following chromatographic steps were performed at room temperature. Twenty milliliter portions of the clarified dialysate were chromatographed on two 5 mL HiTrap-SP cartridges connected in series that had been equilibrated with buffer B. After the sample was applied at 2 mL/min, the cartridges were washed with 20 mL of buffer B and SmtB was eluted with a linear gradient of 0.0−1.0 M NaCl (in buffer B) at 1 mL/min over 30 min. SmtB eluted at approximately 0.8 M NaCl. Fractions were combined (total volume 45 mL) and stored at 4 °C until further purification. Finally, the partially purified SmtB was buffer exchanged using a 5 mL HiTrap Desalting cartridge against buffer E (25 mM Tris, 2 mM DTT, 2 mM EDTA, pH 8.0) and applied to a 2 mL MonoQ column at 0.5 mL/min. SmtB was eluted with a linear gradient of 0−1.0 M NaCl in buffer E at a flow rate of 0.5 mL/min over 20 min. Fractions at approximately 0.3 M NaCl contained SmtB and were combined. The pH of the pooled fractions was adjusted to 6.0, and DTT was added to 1.0 mM for storage at 4 °C. If required, SmtB was concentrated by membrane filtration.

Protein Measurements. Protein concentration in crude bacterial lysate was measured at 260/230 nm according to Kalb and Bernlohr (9). The molar extinction coefficient of SmtB at 280 nm, 5960 M^{-1} cm^{-1} (*10*), was used to measure the concentration of purified SmtB. The progress of purification of SmtB was followed by gel electrophoresis on precast SDS 15% polyacrylamide gels and staining with coomassie R250. The prominent band migrating at M_r of approximately 13 000 Da was indicative of the presence of SmtB. The gels were inspected visually or scanned using SigmaGel software (Jandel Scientific) to estimate the purity of SmtB.

Amino Acid Sequence Analysis. Purified SmtB was subjected to SDS−PAGE and was transferred to a PVDF membrane. The protein then underwent sequence analysis by automated Edman degradation using a Beckman Micro Sequencer, Model PI 2090. The analysis was performed at the Glycoprotein Analysis Core Facility at UAB.

Mass Analysis of Proteins. Mass analysis of purified SmtB was performed using a Perkin-Elmer Sciex Quadrupole mass spectrometer. The analysis was performed by the Comprehensive Cancer Center Mass Spectrometry Shared Facility at UAB.

Sedimentation Equilibrium Analysis. Sedimentation equilibrium analysis was performed in a Beckman XL-A Analytical Ultracentrifuge using a four-cell An-60 Ti rotor. The three cells were loaded with 0.3, 0.5, and 0.8 mg/mL of SmtB, they were centrifuged at 30 000 rpm, and data was gathered at 280 nm. Equilibrium was considered reached when two consecutive sets of data taken 2 h apart were completely superimposable with an rms difference within 0.01 au and showed no systematic deviations. After data at equilibrium had been collected, the rotor speed was increased to 45 000 rpm to deplete the meniscus. This procedure allowed the base line at the meniscus to be measured experimentally.

The buffer used at pH 6.0 contained 25 mM Mes, 2 mM DTT, 2 mM EDTA, and 0.1 M NaCl, while that used at pH 7.4 was made up of 25 mM Tris, 2 mM DTT, 2 mM EDTA, with or without 0.1 M NaCl. The effect of Zn^{2+} on the self-association of SmtB was analyzed at pH 7.4 using the same buffer in which EDTA was replaced with 150 μM $ZnCl_2$. Data was obtained for rotor speeds of 20 000 and 30 000 rpm.

The change in the partial specific volume of SmtB with temperature was taken into account according to the relationship developed by Durchschlag (*11*). Accordingly, the partial specific volume of SmtB was 0.725 and 0.734 $cm^3\ g^{-1}$ at 4 and 25 °C, respectively.

The data-analysis software package of the XL-A allows for a global nonlinear regression of the data obtained from the three centrifuge cells (at various rotor speeds, where relevant) to estimate the monomeric molecular weight and the self-association constant(s). The behavior of SmtB under a given set of conditions was chosen from the best fit analysis of the data to each of the following models: ideal nonassociating monomer, monomer−dimer, monomer−trimer, monomer−tetramer, monomer−dimer−trimer, and monomer−dimer−tetramer association. The final model was chosen such that (1) the estimated monomeric molecular weight was closest to that predicted from the amino acid sequence; (2) the value for the "goodness of fit" (GOF), defined as (degrees of freedom)$^{-1}\sum$(residual/standard error),^{2} was the smallest; and (3) the distribution of error was random about a zero mean (*12*).

Zn^{2+} Binding Analysis. The stoichiometry of Zn^{2+} binding to SmtB was determined by equilibrium dialysis (*13*) at room temperature. An eight-chambered rotary dialysis unit (Hoeffer Scientific Instruments) was used in which each chamber was divided in half by a dialysis membrane. Each of the outer eight compartments contained 200 μL of 37.5 μM SmtB in dialysis buffer (25 mM Tris, 1 mM NTA, 1 mM DTT, 0.1 M NaCl, pH 7.3). Each of the inner compartments contained 200 μL of dialysis buffer containing various amounts of $^{65}ZnCl_2$ in the range 5−100 μM with a specific activity of 13 000 cpm/nmol. The compartments were allowed to equilibrate for 24 h with constant rotation. An aliquot of 150 μL was removed from each compartment, and its radioactivity was counted. Concentrations of bound and free $^{65}ZnCl_2$ were calculated, and the data were fitted by nonlinear least squares to a rectangular hyperbola describing binding of a ligand to its receptor. Data was analyzed with GraphPad PRISM software (GraphPad Software, Inc.).

Table 1: Quality of Least-Squares Analysis for Fitting Sedimentation Equilibrium Data for SmtB at 0.1 M NaCl, pH 7.4, and 22 °C to Various Models

model	monomer MW (Da)	residuals	GOF
ideal monomer	27 509	small, random	0.43
monomer−dimer	13 429	small, systematic	0.51
monomer−trimer	13 400	large, systematic	6.48
monomer−tetramer	11 474	large, systematic	9.24
monomer−dimer−trimer	13 500	small, systematic	0.49
monomer−dimer−tetramer	13 429	small, random	0.41

Sedimentation Velocity Analysis. Velocity experiments were performed to investigate the effect of Zn^{2+} on the sedimentation coefficient of SmtB. The experiments were done at a protein concentration of 1 mg/ml in 25 mM Tris, 2 mM DTT, 0.1 M NaCl, pH 7.40, and 22 °C, with/without 150 μM $ZnCl_2$. The data were analyzed by the time-derivative ($g[s^*]$) method developed by Stafford (*14*).

RESULTS

Expression and Purification of SmtB. Typically, a 24 L culture yielded a wet cell mass of 110 g which yielded 50−100 mg of recombinant SmtB, purified to ≥98% homogeneity as verified by SDS−PAGE overloaded with up to 32 μg of protein per lane. The formation of inclusion bodies during growth was not a problem. During purification it was important to include a thiol reagent to prevent the apparent oxidation of cysteine residues. Higher pH also accelerated denaturation, as shown by formation of an insoluble precipitate upon standing. At pH 6, 2 mM DTT in Mes buffer, the protein was stable for weeks at 4 °C (data not shown). Analysis of the *N*-terminal residues of SmtB gave the sequence TKPVL, in agreement with the published sequence except for the initial methionine. The experimentally determined mass of the protein by mass spectrometry was 13413 Da with only traces of masses at lower or higher values. The DNA-binding properties of the purified protein were tested by EMSA (*2*). The three protein−DNA complexes (C1, C2, and C3) were generated (results not shown).

Quaternary States of SmtB. Data from sedimentation equilibrium experiments at 0.1 M NaCl, pH 7.4, and 22 °C, were fit to all the models described in the methods section (Table 1). The best fit, as judged by the correct estimated monomer molecular weight, small random distribution of residuals, and a low GOF value, was given by the two-step monomer−dimer−tetramer equilibrium model (Figure 1; Table 1). The analysis estimated the monomer−dimer and the monomer−tetramer equilibrium constants, $K_{a(1,2)}$ and $K_{a(1,4)}$, respectively. From that the dimer−tetramer association constant, $K_{a(2,4)}$, was obtained by the relation $K_{a(1,4)}/(K_{a(1,2)})^2$ (*12*). The protein is predominantly dimeric (Table 2).

At pH 7.4 and in the presence of 0.1 M NaCl, there are no appreciable changes in the strengths of the associations on raising the temperature from 4 to 22 °C (Table 2). However, in the absence of NaCl there was about 100-fold

Table 2: Parameters of the Self-Association of SmtB[a]

		4 °C	22 °C	4 °C reverted
pH 7.4	$K_{a(1,2)}$ (M^{-1})	7.96×10^5	3.24×10^5	
		$((7.68-8.25) \times 10^5)$	$((3.04-3.46) \times 10^5)$	
	$K_{a(2,4)}$ (M^{-1})	1.76×10^3	9.90×10^2	
		$((1.57-1.97) \times 10^3)$	$((8.22-11.7) \times 10^2)$	
	monomer MW (Da)	13 416	13 427	
		(13 387, 13 445)	(13 370, 13 486)	
pH 6.0	$K_{a(1,2)}$ (M^{-1})	1.15×10^6	1.52×10^7	1.13×10^6
		$((1.10-1.2) \times 10^6)$	$((1.27-1.83) \times 10^7)$	$((1.08-1.20) \times 10^6)$
	monomer MW (Da)	13 419	13 419	13 421
		(13 337, 13 459)	(13 363, 13 458)	(13 368, 13 499)

[a] Sedimentation equilibrium analysis of SmtB was done in 25 mM Tris or 25 mM Mes, 2 mM DTT, 2 mM EDTA, pH 7.4 or 6.0, respectively. The sedimentation equilibrium data at pH 7.4 were best fit by a monomer−dimer−tetramer model. At pH 6.0, data were best fit to a monomer−dimer model. The numbers in parentheses denote the lower and upper bound of a 95% confidence interval for each estimated parameter. The baseline errors for the three cells as estimated from the fit were nearly identical to the experimental baseline values obtained from meniscus depletion by overspeeding (values not shown).

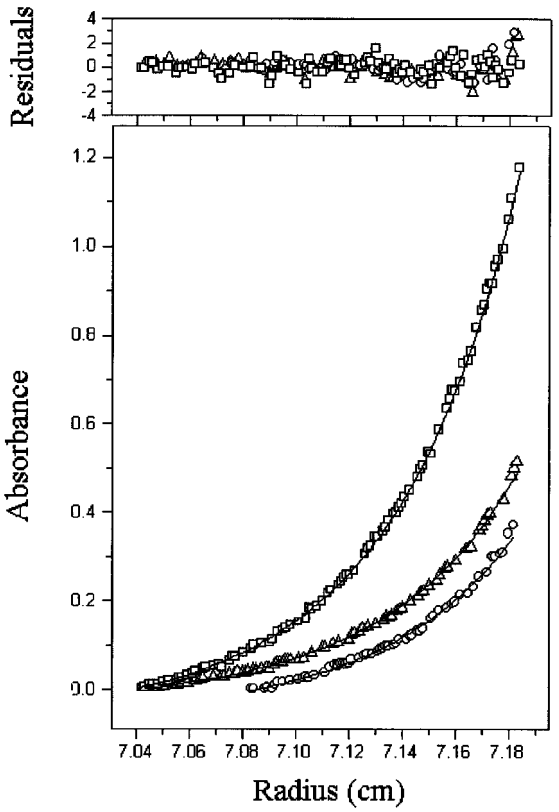

FIGURE 1: Global analysis of the self-association of SmtB under physiological conditions. (Lower panel) Absorption profiles of the radial distribution of SmtB in the three cells. Circles denote data from cell 1 (0.3 mg/mL loading concentration), triangles denote data from cell 2 (0.5 mg/mL loading concentration), and squares are data from cell 3 (0.8 mg/mL loading concentration). The data were fit to a monomer−dimer−tetramer equilibrium model, and the solid lines denote the fitted curves for the three data sets. (Upper panel) The radial distribution of the residuals of the fit. The same three symbols have been used for the three cells. The residual at each radial position has been defined as the ratio of the difference of the measured absorbance and the corresponding fitted value to the standard deviation of the measurement.

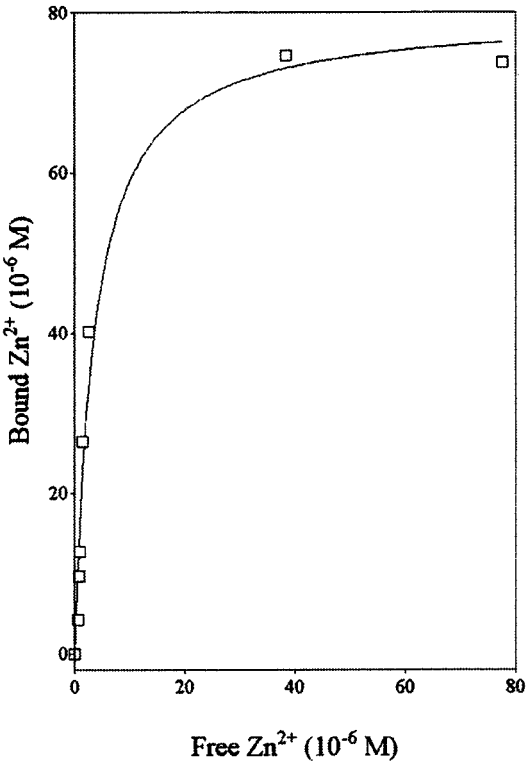

FIGURE 2: The data and the fitted curve from the equilibrium dialysis experiment. The curve denotes the fit to a model of four Zn^{2+} ions binding to a dimer with the same overall binding constant.

decrease in $K_{a(1,2)}$ on raising the temperature from 4 to 25 °C while $K_{a(2,4)}$ remains essentially unchanged (data not shown).

In distinction to results at pH 7.4, data at pH 6.0 fit best a model of monomer−dimer equilibrium. Under the latter condition, there was a reversible 10-fold increase in the association constant on raising the temperature from 4 to 22 °C (Table 2).

Zn^{2+} Binding to SmtB. Data from equilibrium dialysis experiments were fitted to a model with one overall binding constant (Figure 2). Attempts to fit the data to a model with more than one binding constant were unsuccessful. The fit gave a $K_d = (3.49 \pm 0.68) \times 10^{-6}$ M with a maximum binding of $(79.72 \pm 4.45) \times 10^{-6}$ M at infinite metal ion concentration. The goodness of fit R^2 was 0.973. Since the protein monomer concentration was 37.5 μM, there were 2.12 Zn^{2+} ions bound per SmtB monomer.

Effect of Zn^{2+} on SmtB. In the presence of 150 μM Zn^{2+}, SmtB still exhibited a monomer−dimer−tetramer equilibrium in 0.1 M NaCl, pH 7.4, and 22 °C, but the strength of monomer−dimer association now increased about 100-fold, whereas dimer−tetramer association remained essentially unchanged (Table 3). Also, the weight-averaged sedimentation coefficient of the protein increased from 2.00 ± 0.05 to 2.22 ± 0.09 S in the presence of 150 μM Zn^{2+}, an increase

Table 3: Analysis of the Effect of Zn^{2+} Ions on the Parameters for Self-Association of SmtB[a]

	no Zn^{2+}	150 μM Zn^{2+}
$K_{a(1,2)}$ (M^{-1})	5.64×10^5	1.25×10^7
	(5.58×10^5, 6.17×10^5)	(1.24×10^7, 1.26×10^7)
$K_{a(2,4)}$ (M^{-1})	6.31×10^2	1.53×10^2
	(2.75×10^2, 1.22×10^3)	(7.70×10^1, 2.30×10^2)
monomer MW (DA)	13 546 (13 447, 13 660)	13 244 (13 225, 13 264)

[a] Sedimentation equilibrium analysis was done in 25 mM Tris, 2 mM DTT, 0.1 M NaCl, pH 7.4, no EDTA, and at 22 °C. The sedimentation equilibrium data were best fit by a monomer−dimer−tetramer model. The numbers in parentheses denote the lower and the upper bound of a 95% confidence interval for each estimated parameter.

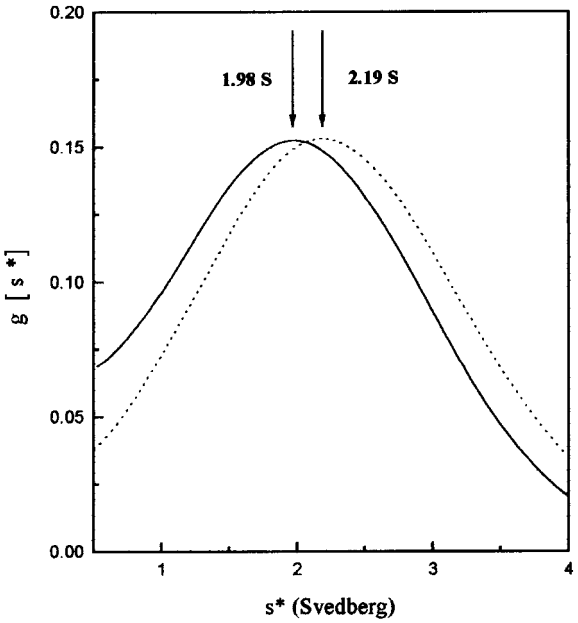

FIGURE 3: Superposition of the $g[s^*]$ profiles of SmtB in the absence (solid line) and in the presence (dotted line) of 150 μM $ZnCl_2$. The arrows with their associated sedimentation coefficient values denote the peak positions of the corresponding gaussians. This result is one of six sets of experiments performed. From these six sets of experiments, the average value of the sedimentation coefficient of SmtB increased from 2.00 to 2.22 S.

greater than that predicted by stronger dimerization alone. The change in sedimentation velocity due to the presence of metal ions was determined using the $g[s^*]$ analysis of the boundary sedimentation data (Figure 3).

DISCUSSION

The cloning strategy and the purification procedure produce large quantities of SmtB. In contrast to recombinant SmtB prepared as a fusion protein (*2*), SmtB produced by the present procedures has no extraneous *N*-terminal amino acids. The predicted size and sequence of the expressed gene product from the *smtB* coding region was verified by mass spectrometry, by SDS−PAGE, and by N-terminal amino acid analysis. It is not surprising that the initial N−terminal methionine is not present, as most proteins produced in *E. coli* are similarly truncated (*15*). The experimentally determined mass of 13 413 Da agrees well with a mass of 13 410 Da calculated from the truncated coding sequence.

At 0.1 M NaCl, pH 7.4, and 22 °C, the repressor exists in a monomer−dimer−tetramer equilibrium, with $K_{a(1,2)} = 3.24 \times 10^5$ M^{-1} and $K_{a(2,4)} = 9.90 \times 10^2$ M^{-1} (Table 2).

Table 4: Estimation of Hydrodynamic Shape of SmtB from Sedimentation Velocity Data

	experimental *s*-value	theoretical *s*-value[a]	$(f/f_{min})^b$	$(f/f_o)^c$	$(a/b)^d$
no Zn^{2+}	2.00 S	2.85 S	1.42	1.16	3.8
150 μM Zn^{2+}	2.22 S	3.09 S	1.39	1.14	3.3

[a] These are the weight-averaged *s*-values assuming the monomer and the dimer as nonhydrated spheres (*17*, *18*). [b] The nonhydrated asymmetry factor (f/f_{min}) is inversely proportional to the ratio of the experimental and the theoretical *s*-values (*19*). [c] The asymmetry factor corrected for hydration at the rate of 0.6 g H_2O/g protein (*20*). [d] The axial ratio of the protein assuming an overall shape of a prolate ellipsoid of revolution (*21*).

Therefore, the dimer is the predominant quaternary state of SmtB under the experimental conditions reported here, with 81% of the protein being in the dimeric form at a protein concentration of 1 mg/mL (75×10^{-6} M), while 16% and 3% of the protein are in monomeric and tetrameric state, respectively. On the other hand, under similar conditions but in the presence of metal ions (Table 3), the repressor is 97% dimeric. It is interesting that other repressors are generally dimeric or tetrameric proteins and their oligomeric structures are believed to be involved in binding to their cognate operator sites (*16*). However, SmtB is inhibited from complexing with its cognate DNA in the presence of Zn^{2+}, under conditions when it is predominantly dimeric.

It is somewhat surprising that the stoichiometry of Zn^{2+} binding reveals two Zn^{2+} ions bound per subunit of SmtB. Attempts to detect two classes of binding sites by curve fitting were unsuccessful. As shown above, SmtB exists predominantly as dimers under the conditions of the equilibrium dialysis experiments. Hence, stoichiometry would indicate four Zn^{2+} bound per dimer of SmtB. This stoichiometry is consistent with the four putative heavy metal binding sites discovered in the SmtB crystal structure (*8*). Computer predictions (*6*) indicating one binding site per subunit could not foresee the sites made by residues at the monomer interface of the dimer. The K_d of 3.49×10^{-6} M is within the range of *in vitro* concentrations of Zn^{2+} which inhibit the binding of SmtB to its cognate DNA to produce complexes C1, C2, and C3 (*2*) and also lies in the range of concentrations of Zn^{2+} which stimulate maximum expression from *smtA* (*4*, *7*).

If the overall hydrodynamic shape of the dimer is assumed to be that of a prolate ellipsoid of revolution, we can calculate an axial ratio (semimajor axis/semiminor axis) of 3.8 from the sedimentation velocity data in the absence of any metal ion at a protein concentration of 1 mg/mL (Table 4). Under the same conditions in the presence of Zn^{2+}, similar calculations predict an axial ratio of 3.3 for the metal-bound repressor (Table 4). This 14% decrease in the axial ratio translates to an overall compaction of the repressor from its conformation in the metal-free state. The increase in the sedimentation coefficient of the repressor from 2.00 to 2.22 S upon metal-binding, therefore, can be accounted for by simultaneous stronger dimerization and change in conformation. This change in conformation could be sufficient to disrupt the geometry necessary for binding of SmtB at the S1/S2 or S3/S4 DNA sites. The fact that the strength of monomer−dimer association at pH 6.0 is about 100-fold higher than that at pH 7.4, both in the absence of Zn^{2+}, may indicate that the contributions of ionic and hydrogen bond

interactions to the subunit association are enhanced by protonation of His residues between pH 7.4 and 6.0. It is interesting that simultaneous mutagenesis of His 105 and 106 (*7*) diminished the ability of Zn^{2+} to initiate transcription controlled by SmtB.

The data presented here are consistent with the proposal that binding of heavy metal ions to SmtB results in stronger self-association and causes a conformational change that triggers the repressor to become more compact. The metal-bound conformation of the free repressor would no longer be capable of forming complexes with DNA, leading to derepression of *smtA*.

ACKNOWLEDGMENT

We sincerely thank Dr. Jarrod Erbe for his gift of the plasmid pJLE3C. We thank Dr. Stephen Barnes for his expertise in mass spectrometry and Dr. John Baker for protein sequencing. We sincerely appreciate the technical guidance with the XL-A analysis software from Drs. Donald McRorie and Michael Johnson. We also thank Rodney Ott, Jr., for assistance with analytical ultracentrifugation.

REFERENCES

1. Morby, A. P., Turner, J. S., Huckle, J. W., and Robinson, N. J. (1993) *Nucleic Acids Res. 21*, 921−925.
2. Erbe, J. L., Taylor, K. B., and Hall, L. M. (1995) *Nucleic Acids Res. 23*, 2472−2478.
3. Silver, S., and Phung, L. T. (1996) *Annu. Rev. Microbiol.* 753−789.
4. Huckle, J. W., Morby, A. P., Turner, J. S., and Robinson, N. J. (1993) *Mol. Microbiol. 7*, 177−187.
5. Turner, J., and Robinson, N. J. (1995) *J. Ind. Microbiol. 14*, 119−125.
6. Shi, W., Wu, J., and Rosen, B. P. (1994) *J. Biol. Chem. 269*, 19826−19829.
7. Turner, J. S., Glands, P. D., Samson, A. C. R., and Robinson, N. J. (1996) *Nucleic Acids Res. 24*, 3714−3721.
8. Cook, W. J., Kar, S. R., Taylor, K. B., and Hall, L. M. (1997) *J. Mol. Biol.*, in press.
9. Kalb, V. F., Jr., and Bernlohr, R. W. (1977) *Anal. Biochem. 82*, 362−371.
10. Pace, C. N., Vajdos, F., Fee, L., Grimsley, G., and Gray, T. (1995) *Protein Sci. 4*, 2411−2423.
11. Durchschlag, H. (1986) in *Thermodynamic Data for Biochemistry and Biotechnology* (Hinz, H.-J., Ed.) pp 45−128, Springer-Verlag, Berlin.
12. McRorie, D. K., and Voelker, P. J. (1993) *Self-Associating Systems in the Analytical Ultracentrifuge*, Vol. II, Beckman Instruments, Inc., Palo Alto, CA.
13. Videen, J. S., Mezger, M. S., Chang, Y. M., and O'Connor, D. T. (1992) *J. Biol. Chem. 267*, 3066−3073.
14. Stafford, W.F., III (1992) in *Analytical Ultracentrifugation in Biochemistry and Polymer Science* (Harding, S. E., Rowe, A. J., & Horton, J. C., Eds.) pp 359−393, The Royal Society of Chemistry, Cambridge, U.K.
15. Lewin, B. (1994) *Genes V*, Oxford University Press, Inc., New York.
16. Silva, J. S., and Silveira, C. F. (1993) *Protein Sci. 2*, 945−950.
17. Teller, D. C., Swanson, E., and De Haen, C. (1979) *Methods Enzymol. 61*, 103−124.
18. Kumosinski, T. F., and Pessen, H. (1985) *Methods Enzymol. 117*, 154−182.
19. Tanford, C. (1961) *Physical Chemistry of Macromolecules*, John Wiley & Sons, Inc., New York.
20. Byron, O. (1997) *Biophys. J. 72*, 408−415.
21. van Holde, K. E. (1985) *Physical Biochemistry*, 2nd ed., Prentice-Hall, Inc., Englewood Cliffs, NJ.

BI971690V